ASSESSMENT OF AVHRR DATA FOR CHARACTERIZING BURNED AREAS AND POST-FIRE VEGETATION RECOVERY

Mário Caetano[1], Leal Mertes[2], Leonor Cadete[1] and José Pereira[3]

1- Centro Nacional de Informação Geográfica (CNIG)
Rua Braamcamp 82-1 Dto, 1200 Lisboa, Portugal.
Tel. 1-3860011, Fax: 1-3862877, e-mail: mario@cnig.pt, leonor@cnig.pt

2-Department of Geography, University of California, Santa Barbara, CA 93106, USA
Tel. 805-8937017 , Fax 805-8933146, e-mail: leal@geog.ucsb.edu

3-Departamento de Engenharia Florestal, ISA, Lisboa, Portugal
Tel. 1 3638161, Fax 1 3645000, e-mail: jmp@rigel.isa.utl.pt

ABSTRACT

A spectral mixture model with image endmembers was applied to an AVHRR image for burned vegetation mapping and assessment of post-fire vegetation recovery in a temperate/semi-arid region. The model converts the reflectance of the two reflective AVHRR bands into proportions of vegetation, soil and burned vegetation at a sub-pixel level. By applying thresholds to the burned fraction, we derived a binary map (burned/unburned), where 67% of the burned pixels were identified. This percentage increased to 91% by applying simple spatial analysis techniques to the output of the spectral mixture analysis. Spectral mixture analysis (SMA) is successful for burned vegetation mapping because the classification of a pixel as burned is based on the abundance of burned vegetation within the area covered by the pixel. This explains why SMA seems more appropriate for burned vegetation mapping, than those techniques that identify burned areas by their low biomass content, e.g. NDVI, that originate confusion between burned areas and bare soil, areas with low vegetation cover or even clear cut areas in multitemporal studies. Preliminary qualitative results show also that spectral mixture analysis is a powerful technique for assessment of vegetation recovery of burned areas.

1. Introduction

Fire is the most important disturbance factor of forests in many parts of the world. The low cost of NOAA (National Oceanic and Atmospheric Administration) AVHRR (Advanced Very High Resolution Radiometer) images, their rapid repeat cycle and coverage of large areas, make them ideal for mapping and monitoring of regional ecosystem properties, such as fire disturbed ecosystem characteristics. One problem that may exist with the use of AVHRR data for burned vegetation mapping is its coarse spatial resolution, even of high spatial resolution imagery (1.1 km at nadir). However, there are several studies that show that, in many parts of the world, the majority of the area burned occurs within a small number of very large fires (Strauss et al., 1989; Chou et al., 1993), and therefore it is reasonable to think that AVHRR data can be used to estimate most of the burned area.

The earlier fire related studies with AVHRR addressed the estimation of the extent of the burned areas together with fire detection. Major contributions to these studies were made through the work of Dozier (1981) and of Matson and Dozier (1981), who presented algorithms to estimate the size and temperature of high temperature sources of subpixel resolution (such as steel plants, gas flares or fires) using channels 3 (reflective/thermal) and 4 (thermal). Commonly, such studies use peak responses of channels 3 data to detect burning areas (e.g. Pereira and Setzer, 1993; Chuvieco and Martín, 1994) and combinations of thermal data to discriminate pixels containing fires (e.g. Flannigan and Vonder Haar, 1986; Kaufman et al., 1990; Lee and Tag, 1990; Langaas, 1992; Kennedy et al., 1994).

Some techniques for the detection and determination of the extent of burned areas with AVHRR data are based on the Normalized Difference Vegetation Index (NDVI) ((Band2 - Band1) / (Band2 + Band1), for AVHRR) (Malingreau et al., 1985; Matson and

Holben, 1987; Frederikesen et al., 1990; Kasischke et al., 1993; Martín and Chuvieco, 1994; Kasischke and French, 1995). The suitability of NDVI for burned vegetation mapping relies on the proportional relation between the NDVI values and green vegetation abundance.

Malingreau et al. (1985) and Matson and Holben (1987) used a single image acquired after the fire(s) events, from a multitemporal dataset, to detect burned areas by their low NDVI values. Kasischke et al. (1993) and Kasischke and French (1995) presented a different approach, based on change detection, where burned areas are identified by a decrease in the vegetation index. This multitemporal approach involved the subtraction of a late summer composited image from an early summer composited image to directly map burn scars. Kasischke et al. (1993) were able to detect 90% of all fires larger than 2000 ha, in the boreal forests of Alaska.

Moreover, the use of AVHRR data to estimate burned area has shown problems related to (1) the confusion between burned areas, bare soil, low vegetation cover and urban areas, and (2) the large area covered by each pixel (1.1 km x 1.1 km) (Matson and Holben, 1987). The confusion with bare soil and urban areas is an artefact of the technique that has been most widely used, i.e. the NDVI, which is only able to detect areas with low vegetation cover or areas experiencing a decrease in vegetation cover when a multitemporal dataset is used (Caetano, 1995). This problem also exists in temperate and semi-arid regions if the thermal channels are used, since areas with no or low vegetation have similar thermal characteristics to burned areas. On the other hand, the large AVHRR pixels can encompass burned and unburned areas, resulting in difficulties in estimating the actual percentage area of each pixel that is burned, leading to under- or overestimates of burned areas.

The method we use, spectral mixture analysis (SMA) (Smith et al., 1990), addresses directly the problem of the mixed pixels and of the confusion with other land cover types, since the satellite data are converted into proportions of vegetation, soil, and burned vegetation. SMA has already been successfully tested with AVHRR data as a technique to extract agricultural information (Quarmby et al., 1992) and forest information (Cross et al., 1991). At a finer spatial resolution, i.e. using Landsat Thematic Mapper (TM) data, SMA proved to be an adequate technique for mapping spatial patterns of burned severity (Caetano et al., 1994). We also use a simple spatial analysis technique to improve the results from the application of a spectral mixture model to avoid confusion between partially burned pixels from the year of the image acquisition, and areas burned in previous years. This study is the first attempt to use SMA with AVHRR images for burned vegetation mapping. The model is tested in Portugal. It is also important to say that this study is one of the first to use AVHRR data for burned vegetation mapping in temperate and semi-arid regions, since most of the studies were carried on tropical and subtropical areas (Matson and Holben, 1987; Kaufman et al., 1990; Malingreau et al., 1985; Malingreau, 1990; Pereira and Setzer, 1993; Kennedy et al., 1994) and in boreal forests (Kasischke et al., 1993; Kasischke and French, 1995). For testing the potential of AVHRR data for post-fire vegetation recovery assessment we carried out preliminary studies, where we compared the vegetation fraction of one Landsat image which was acquired 10 days after a large fire, with the vegetation fraction of one AVHRR image that was acquired 14 months later.

2. Study area and dataset

Portugal is the study area selected to apply and test the methodology because of its typical temperate and semi-arid bio-climatic characteristics. Therefore, the results from this study can be generalized to other temperate and semi-arid bio-climatic regions where fire has been the most important disturbing factor of forest ecosystems and where studies on burned vegetation mapping with AVHRR data are scarce.

We used a cloud-free NOAA-11 AVHRR image, in High Resolution Picture Transmission (HRPT) format, obtained from the Satellite Data Receiving Station at the University of Dundee. These data relate to the five AVHRR/2 channels (channel 1: 0.58-0.68 μm; channel 2: 0.725-1.1 μm; channel 3: 3.55-3.93 μm; channel 4: 10.3-11.3 μm and channel 5: 11.5-12.5μm) of an early afternoon pass from the 16th of September 1991. Nadir observations have a cell resolution of 1.1 km x 1.1 km.

For burned vegetation mapping accuracy assessment we used existing digital data on burned areas from the 1991 forest fire season, at a scale of 1: 100 000 (in Transverse Mercator projection), available from the Portuguese Forest Service (IF - Instituto Florestal), who plot every fire scar larger than 12.5 ha. This map, hereafter referred to as the IF reference map, was generated from visual analysis of Landsat TM imagery colour composites followed by on-screen digitizing of burned areas. All fires occurring after

the AVHRR image acquisition date were removed from the analysis, as well as all burned areas smaller than 180 ha (approximately 1.5 pixels in an AVHRR image). Moreover, in the assessment stage the study area was confined to Central Portugal, as IF data used proved to be more reliable for this part of the country. We used the CORINE landcover digital database to tackle some problems that could not be solved by spectral mixture analysis. For this purpose we used a raster transformed CORINE landcover map existing at CNIG, Portugal (Centro Nacional de Informação Geográfica), with 275 m x 275 m pixel resolution (Cadete, 1996).

For studying vegetation recovery on burned areas based on SMA of AVHRR images, we used endmember fraction images generated by Caetano et al. (1994) from Landsat TM data for one large fire (9000 ha) that occurred in July, 1990 in Central Portugal. These images were compared with the fraction images generated in this study using AVHRR data.

3. Methods

The NOAA AVHRR image was registered to the Transverse Mercator projection by applying an indirect navigation correction based on a precise orbital model developed at the Colorado Center for Astrodynamics Research (CCAR) (Rosborough et al., 1994). Since there were still some deviations between satellite imagery and the reference map projection grid, image geometry was further refined applying a 2nd. order model and nearest neighbour resampling. Radiometric calibration was also applied during the process, converting digital counts into top of atmosphere reflectances (channels 1 and 2) and brightness temperatures in Kelvin degrees, corrected for non-linear effects (channels 3, 4 and 5). The gain and offset coefficients for the reflective channels were updated using piecewise linear fits (Teillet and Holben, 1994), instead of using the pre-launch default options available in the CCAR software which have problems of temporal drift.

The method to extract information on burned areas from the AVHRR image is based on the generation of a spectral mixture model, which consists of expressing each pixel as a linear combination of pure spectra, i.e. endmembers, extracted from the image (Adams et al., 1986; Smith et al., 1990). The output from the model is a fraction image for each endmember, where the spectral contribution of the endmember is retained for each pixel. Since the spectral contribution of a given endmember is related to the abundance of the endmember, the output of the model is related to the abundance of the endmember in the area covered by each pixel.

In order to identify burned areas from the year of image acquisition and to evaluate the recovery of vegetation of burned areas from previous years, three endmembers are necessary to build the spectral mixture model, i.e. vegetation, soil and burned vegetation. Because of the way the model is set up, three bands are necessary. We decided to use band 1 (red) and band 2 (near infrared) because they are useful to identify burned areas, as it has been reported in several studies and as it was checked in our study area. The channels 3, 4 and 5 were not used in the model because the signal of burned areas and of bare soil or areas with low vegetation cover in these channels are very similar. On the other hand, we are not familiar enough with these channels to assume that they mix in a linear way. However, with just two bands and three endmembers (i.e. the number of endmembers exceeds the number of bands in one) the model would be saturated and there would be no degrees of freedom to gauge performance (the corresponding residuals would be zero). For this reason we decided to use one additional band, the NDVI. We also think that the inclusion of a band ratio in the model is helpful to reduce topographic effects on the satellite signal, especially since we are not using a shade endmember to take into account the variations in lighting geometry. We checked for correlation problems between the NDVI and the two AVHRR channels used in the model and we verified that the correlation coefficient between NDVI and each of the bands was much lower than the correlation between the two bands.

The burned endmember was selected in the core of a large burned area, known not to have unburned islands, to avoid contamination with unburned vegetation which may happen in small burned areas and at the boundaries of large fires. On the other hand, to guarantee that the charred timber and charcoal residue would be abundant, we checked on the CORINE map that the land-cover of the area before the fire was a dense forest. The last requirement that we imposed on the selection of burned endmembers was that the area had to have been burnt just a few days before the image acquisition date, in order to guarantee that there would be charcoal covering the soil at the time of image acquisition. This also meant that there was not logging of burned timber or runoff of ashes in the time-lapse between the fire occurrence and the image acquisition. The vegetation endmember was selected

from a mature pine stand and the soil endmember was selected from a large bare soil area that was not burned in previous years, in order to avoid contamination by charcoal.

To build the model we used a least squares method, with the constraint that the endmember fractions in each pixel should add up to one. To assess the model we used (1) the overall RMS (root mean squared error), (2) the RMS image, and (3) the spatial patterns in the fraction images. The root-mean-squared error (RMS) is a measure of the spectra residuals that cannot be explained by the mixture model, and it is based on the difference between the measured reflectance and the reflectance as estimated by the model. The RMS value for each pixel, was used to generate one image. Because we did not use the constraint that the endmember fractions should be non-negative and larger than one, fractions under zero (underflow) or greater than one (overflow) can be used as an indicator that the model is not well fitted to the data.

The selection of image endmembers is an iterative procedure. The fraction images and the RMS image are used for selection of the best image endmembers, i.e., the endmembers that best model the image. In each run of the model, the analyst may define new endmembers or use different pixels or set of pixels to define endmembers already identified. The goal is to find those endmembers that best model the data.

For burned vegetation mapping based on SMA of AVHRR images, we used two different methods: the Spectral Mixture Analysis based Method (SMAbM) and the Spectral Mixture Analysis followed by Spatial Analysis Method (SMAfSAM). The SMAbM generates a binary map, burned /not-burned, by setting a threshold to the burned fraction image. The SMAfSAM is based on a methodology developed by Caetano (1995) and it generates a map with 3 classes, burned, not-burned and partially burned areas, by setting thresholds to the burned fraction image, followed by spatial analysis to identify the partially burned pixels that could be classified as burned (SMAfSA). This spatial analysis was performed within a GIS, and it consists of the following steps: (1) build a 1.1 km buffer around the burned pixels, (2) identify the partially burned pixels that are within the 1.1 km buffer and classify them as burned, and (3) identify the ones outside the buffer and classify them as unburned. We also combined the SMA output in RGB colour composites by assigning each endmember to one of the RGB colour guns, to help in the interpretation of the SMA output.

To improve the results of the spectral mixture analysis we used a transformed CORINE landcover digital database with 275 m x 275 m pixel resolution to identify urban areas and water bodies, since these areas were not well modelled by the selected endmembers, and no more endmembers could be added to the model because of the number of bands used in the model. In this database, after identifying the urban areas, water bodies and wetlands, we resampled the cells to 1.1 km x 1.1 km, to match the size of the SMA outputs, with a special procedure to keep linear features, such as rivers. The urban and water mask was then applied to the SMA output.

To assess the potential of SMA of AVHRR images to detect post-fire vegetation recovery we compared the vegetation fraction of this study to the vegetation fraction image generated by Caetano et al. (1994) from Landsat-TM data for one large fire (9000 ha) that occurred in July, 1990 in Central Portugal. The TM fraction images were spatially degraded within a GIS to generate AVHRR size pixels.

The accuracy assessment of the burned areas classification was done with error matrices, for an area in Central Portugal (76 km x 64 km), where several fires occurred in the summer of 1991. In these matrices the number of observations assigned to a given class are compared to the IF reference map. The IF fire scar map was used in a vector format for visual analysis of the accuracy assessment, and it was converted to a 1.1 Km^2 cell to compare it with the results of the SMA analysis. To summarise the classification accuracy we used three indices: PCC (percentage of pixels correctly classified), OME (percentage of omission errors) and COME (percentage of commission errors). The PCC for a given class is defined as the number of pixels that were correctly classified in relation to the total number of pixels of that specific class on the reference map. Because this index only takes into account the correctly classified pixels and the omission errors (pixels that were incorrectly assigned to other classes), we also calculated the percentage of commission errors (COME) for each class, which is the number of pixels that were incorrectly assigned to this class divided by the total number of pixels of this class on the reference map. The OME was also calculated. For a given class, the OME is the number of pixels that were incorrectly assigned to another class divided by the number of pixels of the class (to which the OME is calculated) on the reference map. All these indices were calculated at a class level. An overall accuracy index could not be used, because it would be biased by the large percentage of unburned

area in the test area (89%) when compared to that of area burned (11%).

4. Results and discussion

The model assessment was based on the RMS and on the endmember fraction images. A low overall RMS (1.17), low RMS´s at a pixel level (always smaller than 2) and insignificant over- and under-flow indicate that the endmembers were all chosen and they account well for the spectral variation of the data. We also verified that there were no trends in the RMS and fraction images indicating that parts of the image were poorly modelled because of atmospheric variations across the study area, which would be expected because of the size of the study area. However, we verified that the endmembers that were chosen were not able to model urban areas and water bodies, which makes sense since we did not use any urban or water endmembers. Water bodies and wetlands were characterized by a large proportion of the burned endmember. The urban areas were modelled as a combination of all endmembers. In fact, both of these two landcover types were identified by the model assessment techniques, large RMS, and large under- and over-flows. To avoid confusion of landcover types in the final maps we applied an urban and water mask to the SMA output, as described in the methods section.

The burned areas map generated by setting a threshold (60%) to the burned fraction (SMAbM) and the one improved with spatial analysis (SMAfSAM) are presented in plate_. We overlaid the IF reference map, in vector format, onto the classified images. The error matrices and the classification accuracy indices (PCC, OME and COME) are presented in table 1.

Table 1 - Error matrix and accuracy assessment indices (PCC, COM e OME) of two burned area maps generated with two methodologies: (1) method based on setting a threshold to the burned fraction (SMAbM), and (2) method improved with spatial analysis (SMAfSA). Note that the second parcel of the burned class in the SMAfSA confusion matrix (103 and 176) corresponds to the partially burned areas classified as burned with spatial analysis. These were classified as unburned in the SMAbM method.

		Classified image (SMAbM)		Classified image (SMAfSAM)		Total
		Burned	Unburned	Burned	Unburned	
IF Ref. Map	Burned	295	144	(295 + 103)	41	439
	Unburned	77	3486	(77 + 176)	3310	3563
Total		372	3630	651	3351	
	PCC (%)	67	98	91	93	
	OME (%)	33	2	9	7	
	COME (%)	18	4	58	1	

From the analysis of table 1 the following observations can be made:

(1) both methods generated maps where the two classes, burned and unburned, were satisfactorily assessed. In fact all the PCC were larger than 90%, except the PCC of the burned class in the SMAbM (67%);

(2) the SMAfSAM generated a map with a better accuracy (91% of the pixels were correctly classified as burned) compared to the one just based on SMA;

(3) the unburned area was identified with a slightly better accuracy with the SMAbM (PCC is 98%) than with the SMAfSA (PCC is 93%);

(4) in the maps generated by SMAfSA the burned class has large commission errors (COME is 58%).

In the map generated by the SMAfSAM (plate_) we divided the burned class in the class of the pixels that were completely burned (burned area) from the ones that were partially burned, and that were identified by spatial analysis (partially burned areas). Table 1 for the SMAfSAM confusion matrix, also discriminates these two classes (burned and partially burned areas), so that the table could be related to the maps.

The burned area class encompasses the pixels with a very large proportion of the burned endmember. The pixels of this class show up mainly in the core of the burned areas, which makes sense since this is where it is most likely to find pixels covering just burned

area with small proportions of vegetation and soil. An iterative process was used to establish the burned fraction threshold (60%), so that only burned areas could be selected. This threshold may seem too low, however, it must be stressed that this value is related to the purest burned pixel in the image and not to pure burned material itself. In fact, even a pixel covering an area completely burned will always have a soil signal. This low threshold reflects the difficulty on finding pure burned pixels in an AVHRR image, due to the large area covered by each pixel.

From the analysis of the two maps we can say that not only the agreement of the reference map is much larger in the SMAfSA map (plate 1), but also that the shape of the burned areas are identified more satisfactorily in the SMAfSA. The reason for this is related to the small burned areas and to the boundaries of the large burned areas that were classified as burned in the SMAfSAM and as unburned vegetation in the SMAbM. The pixels of partially burned areas, which are a mix of vegetation, burned vegetation and soil, could not be automatically classified as burned, because they also encompass burned areas from previous years. The current year partially burned areas correspond to areas where the fire did not burn all the vegetation or where there was a large proportion of exposed soil before the fire occurrence. The intermediate values of the fraction endmembers in the areas that were burned in previous years are due to runoff of the charcoal residue, which causes a decrease in the burned fraction and an increase in the soil fraction, and also to vegetation recovery, which causes an increase in the vegetation fraction. Spatial analysis was the strategy followed to discriminate the partially burned areas of that year from areas that were burnt in previous years. We assumed that partially burned areas contiguous to areas burned in the current year could be classified as burned, and the ones that were not contiguous to any burned area could be classified as unburned vegetation. However, the spatial analysis is not able to discriminate those areas that were burned in previous years but that are contiguous to areas that burned during the current year. These areas will be classified as partially burned and they will introduce an error in the final product.

We also identified that most of the unburned pixels that were classified as burned by the SMAfSAM (expressed in the large COME of the burned area class) are the partially burned pixels of the boundaries of the burned areas. It is reasonable to assign some of these errors to the lack of precision on the delimitation of the burned areas in the IF reference map, as mentioned by Cadete (1996). On the other hand, the conversion of the IF reference map to 1.1 km cell grid map, also created some spatial errors.

Another pertinent comment regards the size of the burned areas that were identified. In fact, fire scars as small as 240 ha (2 pixels) were successfully identified by simple thresholding of the burned fraction (plate 1).

In plate 2 we present a RGB colour composite of the endmember fraction images of an area in Central Portugal, where each endmember, i.e. burned vegetation, vegetation and soil, were assigned respectively to the red, green and blue colour guns. The black polygons over the image are the burned areas from the IF reference map. This figure clearly shows the information that is lost when one uses the SMA output from an automatic classification. In fact, a simple visual analysis allows identification of the burned areas of the current year, as well as the areas that were burned in previous years. In this figure, one can see that most burned areas show up in red, because of the large proportion of the burned fraction (burned area class in plate 2). The boundaries of the burned areas are not so reddish as the core because these pixels are contaminated by unburned vegetation (partially burned areas in plate 1). Unburned vegetation shows up in green, with different amounts of blue depending on the relative proportion of soil. Areas that were not burned in the same year as that of image acquisition show up with some red, because of burned timber that still remains in the area covered by the pixel.

This image is also appropriate to show the advantages of using SMA over the NDVI for burned vegetation mapping. When NDVI is used, burned areas are identified by low biomass content. For this reason, low NDVI values also identify landcover types that are not burned, but that have low biomass content, e.g. bare soil, areas with low vegetation because of climatic characteristics or because of clear cuts (blue pixels in plate 2). The method based on SMA, identifies the burned areas by their large abundance of burned material in the area covered by the pixel, and therefore there are no confusions with other landcover types with low biomass content. The relation between NDVI and SMA can also be expressed by the correlation coefficients. The correlation coefficient between the NDVI image and the vegetation fraction is very high (0.99), when compared to the correlation between NDVI and the burned fraction (-0.44). Even in multitemporal studies using the NDVI, where burned areas are

identified by a decrease in the vegetation cover, fire scars are confused with areas that have been clear cut. Another difference between the two approaches, NDVI and SMA, for burned vegetation mapping is that SMA does not require more than one image to identify burned areas with a satisfactory accuracy, while the techniques for burned vegetation mapping based on NDVI require the use of more than one image.

For studying the potential of methods based on SMA for assessment of vegetation recovery in burned areas, we studied an area that was burned 1 year before, July 1990, and which is delineated in yellow in plate 2. We subtracted the vegetation fraction as estimated by SMA on one Landsat image from 10 days after a large fire (Caetano et al., 1994) to the vegetation fraction as estimated by SMA on the AVHRR image. This difference image is shown in figure 1. As expected, within the boundaries of the fire (central part of the image) there was an increase in the vegetation fraction (brightest pixels).

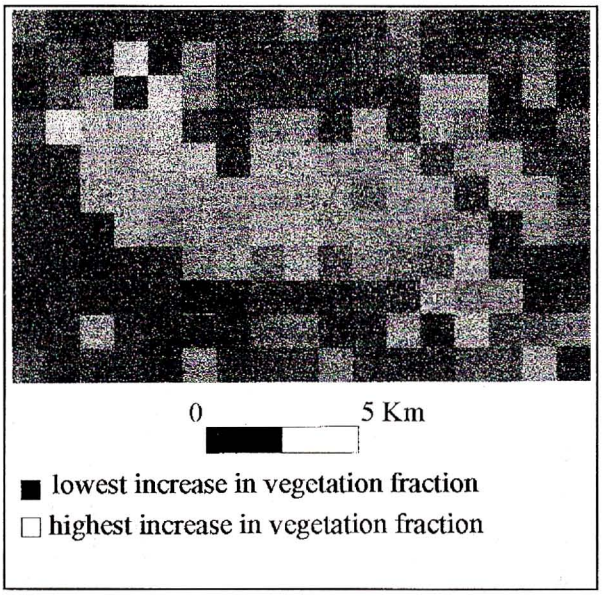

Figure 1 - Difference image of the vegetation fractions as extracted from the 1991 AVHRR image and from a 1990 Landsat image.

See plate IX at end of volume

The vegetation recovery evaluation has to be qualitative, since the fraction images from the two satellite images cannot be quantitatively compared because the model was built with image endmembers, which means that the proportions of the endmembers are relative to the pixels that were used to model the image. If the pixels are not completely pure (which may happen in the AVHRR image) a given percentage of vegetation, for example, does not mean that the pixel is covered by the same proportion of vegetation. On the other hand, the fraction images from July were normalised, i.e. images where the shade fraction was removed, and the AVHRR fraction images were not normalised because no shade endmember was used. Therefore the AVHRR output proportions cannot be directly linked with the abundance of the material on the ground and consequently they cannot be quantitatively compared with the TM fractions. Besides these problems associated with SMA, there are also errors introduced by the spatial degradation of the Landsat vegetation fraction to match the AVHRR pixel size. Despite all these limitations, these results show that SMA is able to detect subtle increases in the vegetation cover, as shown in figure 1.

5. CONCLUSIONS

A linear mixture model was applied to an AVHRR image of Portugal for burned vegetation mapping and vegetation recovery assessment in burned areas of previous years. The output of the model is a fraction image, where the proportion of the endmember used to model the image, i.e. vegetation, soil and burned, is retained or assigned to each pixel. A binary map burned/unburned was derived by applying a threshold to the burned fraction generated by the model. The results were improved by simple spatial techniques within a GIS. The results presented in this study suggest that assessment of burned areas (larger than 500 ha) in temperate and semi-arid regions can be done in an inexpensive, rapid and accurate way with AVHRR images by using spectral mixture analysis and consequently provide national governments and national Forest Services with timely data on burned areas (spatial distribution and extent of burned land). The main conclusions from this study can be summarised as follows:

(1) Automatic classification based on thresholds of the burned fraction generate burned area maps where 67% of the burned pixels (core of burned areas) were correctly classified.

(2) Spatial analysis within a GIS after applying the threshold to the burned fraction generated a map where 91% of the burned pixels were identified. This improvement is due to the fact that partially burned pixels located in the boundaries of the current year large fires were classified as burned, without confusion with areas that were burnt in previous years.

(3) Urban areas, water bodies and wetlands could not be discriminated from burned areas and partially

burned areas. This is a consequence of not using urban and water endmembers to build the model. These areas were masked out by using the CORINE landcover map.

(4) The improved technique was able to identify small fires (the area of the smallest fire that was identified was two pixels) without any errors.

(5) When compared to the NDVI approach, the spectral mixture analysis seemed more reliable for burned vegetation mapping, since it is based on the proportion of burned vegetation within each pixel, and not on low NDVI values (low vegetation cover). For this reason, in the SMA burned area maps there are no confusions that may exist in a burned areas map based on the NDVI, such as the confusions between burned areas and areas with low vegetation cover.

(6) Even though recent studies of burned vegetation mapping with AVHRR data based on the NDVI require the use of more than one image (before and after the fire season) to generate maps with satisfactory accuracy, we proved in this study that if spectral mixture analysis is used, a single image is sufficient to produce maps with satisfactory accuracy. It should be noted that we used a cloud free, close to nadir image.

(7) Visual analysis of RGB colour composites with the endmembers fractions proved to be a powerful tool for a preliminary analysis of burned areas in the study area. Burned areas, bare soil, areas with low vegetation cover and areas that burned in previous years could be discriminated.

(8) Preliminary and qualitative results show that SMA of AVHRR images has good potential for vegetation recovery assessment.

As future research guidelines regarding burned vegetation mapping and vegetation recovery assessment with AVHRR images, using spectral mixture analysis, we suggest (1) the use of reference endmembers collected in the field with a radiometer, and (2) the use of a shade endmember to take into account the lighting geometry variations. Smith et al. (1990) and Caetano (1995), among others, showed the importance of the shade endmember for removing the topographic effect in satellite images. A spectral mixture model with reference endmembers which integrates a shade endmember would make it possible to:

(1) Make a direct relationship between the proportion of each of the endmembers and the abundance of the material on the ground surface, since each endmember would be a pure component and the topographic effect could be removed by image normalisation in relation to the shade endmember (Smith et al., 1990, Caetano, 1995). This would allow the estimation of the pixel percentage that is burned and, consequently, a more detailed map of the boundaries of the burned areas. It should be noted that this is not possible with image endmembers since it is very hard to guarantee that the pixels used as endmembers are 100 % occupied by pure landcover classes. Therefore, when image endmembers are used, the fraction images of the endmembers are not the absolute abundance of the endmembers on the ground. On the other hand, if reference endmembers were used and shade effects removed, the threshold to apply to the burned fraction to identify the burned areas could be used in any AVHRR image.

(2) Make a quantitative comparison of endmember fractions from different images and subsequently a more precise vegetation recovery assessment or soil loss evaluation by erosion processes in burned areas.

Further research work to test the robustness of the methodology should be done, including: (1) definition of the minimum burned area that SMA can identify in AVHRR data, and (2) quantitative analysis, based on field work, to assess the classification of recovering burned areas.

This work was done while the first author was a visiting scholar in the Department of Geography, University of California, Santa Barbara, USA, funded by JNICT (PRAXIS XXI/BD/2641/94). Participation of the first author takes place under EC project AAIR-CT94-2392. Participation of the fourth author takes place under JNICT project STRDA/C/AMB/762/92.

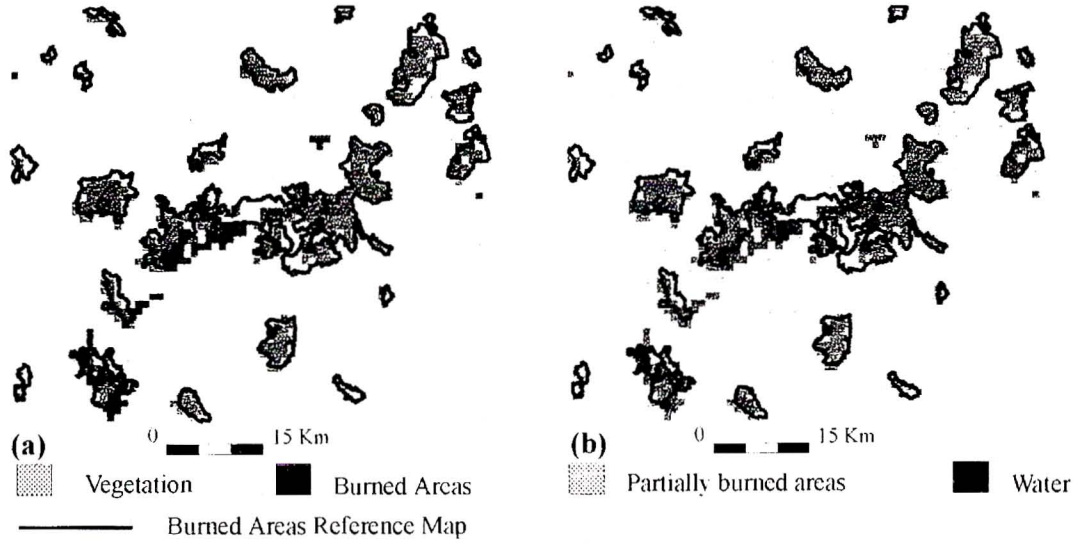

Plate 1 - Maps of burned areas of Central Portugal derived from a 16 September, 1991. AVHRR image: (a) by setting a threshold to the burned fraction (SMAbM); (b) by setting a threshold to the burned fraction, followed by spatial analysis (SMAfSA). The IF burned areas reference map is represented by black lines

See Plate X at end of volume

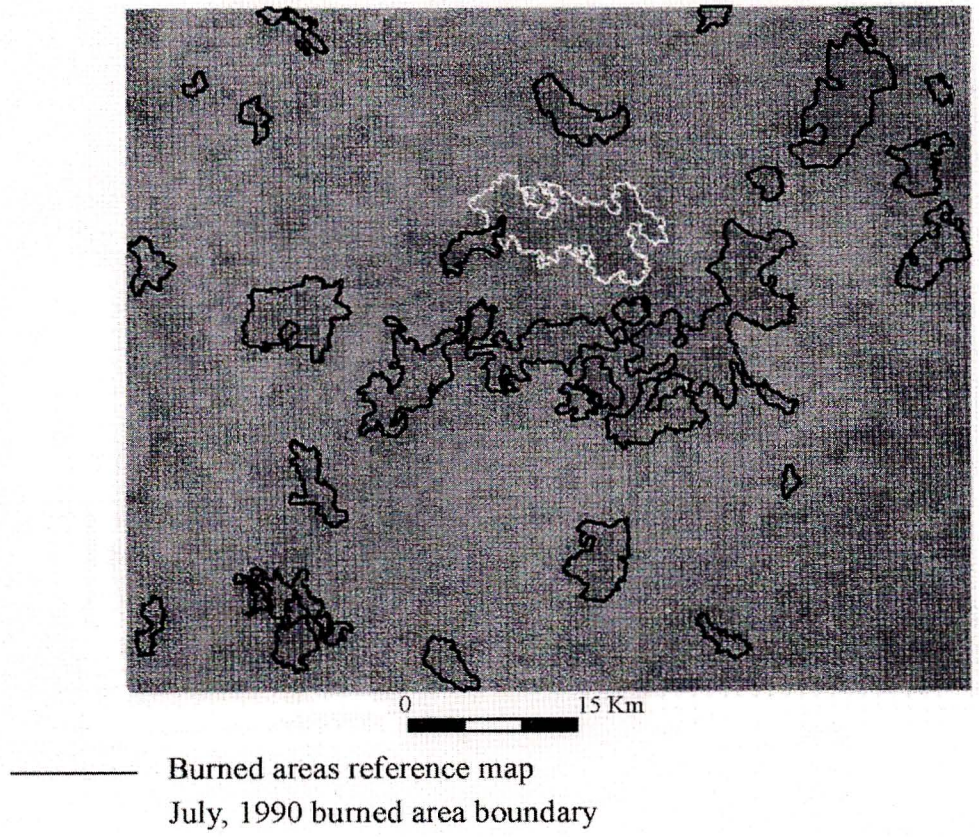

Plate 2 - RGB colour composite of Central Portugal with fraction images generated by the application of a spectral mixture model to a 16 September, 1991. AVHRR image (Red - burned fraction; Green - vegetation fraction; Blue - soil fraction). The IF burned areas reference map is represented by black lines and a large fire that occured 1 year before (July, 1990) is deimited by a yellow line

See Plate X at end of volume

REFERENCES

Adams, J. B., M. O. Smith, and P. E. Johnson (1986). Spectral mixture modeling. A new analysis of rock and soil at the Vicking Lander I site. Journal of Geophysical Research 91: 8098-8812.

Cadete, L. (1996). Utilização de dados NOAA AVHRR HRPT na localização e estimação de áreas ardidas em floresta portuguesa. Centro Nacional de Informação Geográfica. Internal report.

Caetano, M. (1995). Burned vegetation mapping in mountainous areas with satellite remote sensing. MA thesis, University of California, Santa Barbara. 328 pp.

Caetano, M., L.A.K. Mertes, and J.M.C. Pereira (1994). Using spectral mixing for fire severity mapping. Proceedings of the 2nd International Conference on forest fire research. Coimbra, Portugal, 21 - 24 November, 1994, vol. 2, 667-677.

Chou, Y.H., R.A. Minnich, and R.J. Dezzani (1993). Do fire sizes differ between Southern California and Baja California. Forest Science, 39, 835-844.

Chuvieco, E. , and M.P. Martín (1994). A simple method for fire growth mapping using AVHRR channel 3 data. International Journal of Remote Sensing, 15, 3141-3146.

Cross, A.M., J.J. Settle, N.A. Drake, and R.T.M. Paivinen (1991). Subpixel measurement of tropical forest cover using AVHRR data. International Journal of Remote Sensing, 12, 1119-1129.

Dozier, J. (1981). A method for satellite identification of surface temperature fields of subpixel resolution. Remote Sensing of Environment, 11, 221-229.

Flannigan, M.D., and T.H Vonder Haar (1986). Forest fire monitoring using NOAA satellite AVHRR. Canadian Journal of Forest Research, 16, 975-982.

Frederikesen, P., S. Langaas, and M. Mbaye (1990). NOAA/AVHTT and GIS-based monitoring of fire activity in Senegal - a provisional methodology and potential applications, in Fire in Tropical Biota, edited by J.G. Goldammer (Berlin:Springer-Verlag), pp. 400-417.

Kasischke, E.S., and N.H French (1995). Locating and estimating the areal extent of wildfires in Alaskan boreal forests using multiple-season AVHRR NDVI composite data. Remote Sensing of Environment, 51, 263-275.

Kasischke, E.S., N.H. French, P. Harrel, N.L. Christensen, S.L. Ustin, and D. Barrin (1993). Monitoring of wildfires in boreal forest using large area AVHRR NDVI composite image data. Remote Sensing of Environment, 45, 61-71.

Kaufman, Y., A. Setzer, C. Justice, C.J. Tucker, and I. Fung (1990). Remote sensing of biomass burning in the tropics, in Fires in Tropical Biota, edited by J.F. Goldammer (Berlin:Springer-Verlag), pp. 371-399.

Kennedy, P.J., A.S. Belward, and J-M. Gregoire (1994). An improved approach to fire monitoring in West Africa using AVHRR data. International Journal of Remote Sensing, 15, 2235-2255.

Langaas, S. (1992). Temporal and spatial distribution of savanna fires in Senegal and the Gambia, West Africa, 1989-1990, derived from multi-temporal AVHRR images. International Journal of Remote Sensing, 2, 21-36.

Lee, T.F., and P.M. Tag (1990). Improved detection of hotspots using the AVHRR 3,7 μm channel. Bulletin American Meteorological Society, 71: 1722-1730.

Malingreau, J.-P., G. Stevens, and L. Fellows (1985). The 1982-83 forest fires of Kalimantan and North Borneo. Satellite observations for detection and monitoring. Ambio, 14, 314-321.

Malingreau, J.-P. (1990). The contribution of remote sensing to the global monitoring of fires in tropical and subtropical ecosystems, in Fire in Tropical Biota, edited by J.G. Goldammer (Berlin:Springer-Verlag), pp. 337-370.

Matson, M., and J. Dozier (1981). Identification of subresolution high temperature sources using a thermal IR sensor. Photogrammetric Engineering and Remote Sensing, 47, 1311-1318.

Matson, M., and B. Holben (1987). Satellite detection of tropical burning in Brazil. International Journal of Remote Sensing, 8, 509-516.

Martín, M. P., and E. Chuvieco (1994). Mapping and evaluation of burned land from multitemporal analysis of AVHRR NDVI images. Proceedings of the International Workshop on Satellite Technology and GIS for Mediterranean Forest Mapping and Fire Management. Thessaloniki, Greece. 4 - 6 November, 1993, 71-83.

Pereira, M.C., and A.W. Setzer (1993). Spectral characteristics of deforestation fires in NOAA/AVHRR images. International Journal of Remote Sensing, 14:583-597.

Quarmby, N. A., J. R. G. Townshend, J. J. Settle, and K. J. White (1992). Linear mixture modeling applied to AVHRR data for crop area estimation. International Journal of Remote Sensing. 13, 415-425.

Rosborough, G.W.; D.G. Baldwin, and W.J. Emery (1994). Precise AVHRR image navigation. IEEE Transactions on Geoscience and Remote Sensing, 32, 644-657.

Smith, M. O., S. L. Ustin, J. B. Adams, and A. R. Gillespie (1990). Vegetation in deserts: I. A regional measure of abundance from multispectral images. Remote Sensing of Environment 31, 1- 26.

Strauss, D., L. Bednar, and R. Mees 1989, Do one percent of fires cause ninety-nine percent of the damage?. Forest Science, 3, 319-328

Teillet, P.M., and B.N. Holben (1994). Towards operational radiometric calibration of NOAA AVHRR imagery in the visible and near-infrared channels. Canadian Journal of Remote Sensing, 20, 1-10.